Geophysical Research Letters

RESEARCH LETTER
10.1029/2024GL109460

# The Calm and Variable Inner Life of the Atlantic Intertropical Convergence Zone: The Relationship Between the Doldrums and Surface Convergence

**J. M. Windmiller**[1]

[1]Max Planck Institute for Meteorology, Hamburg, Germany

**Key Points:**

- The doldrums are confined to the area of time-mean convergence of the Atlantic Intertropical Convergence Zone (ITCZ)
- The frequency distribution of low wind speed events peaks between the edges of the ITCZ, which are characterized by increased convergence
- Low wind speed events within the ITCZ occur when precipitation is absent, suggesting they coincide with local low-level divergence

**Supporting Information:**

Supporting Information may be found in the online version of this article.

**Correspondence to:**

J. M. Windmiller,
julia.windmiller@mpimet.mpg.de

**Citation:**

Windmiller, J. M. (2024). The calm and variable inner life of the Atlantic Intertropical Convergence Zone: The relationship between the doldrums and surface convergence. *Geophysical Research Letters*, *51*, e2024GL109460. https://doi.org/10.1029/2024GL109460

Received 24 MAR 2024
Accepted 17 JUL 2024



**Abstract** The doldrums are regions of low wind speeds and variable wind directions in the deep tropics that have been known for centuries. Although the doldrums are often associated with the Intertropical Convergence Zone (ITCZ), the exact relationship remains unclear. This study re-examines the relationship between low-level convergence and the Atlantic doldrums. By analyzing the frequency distribution of low wind speed events in reanalysis and buoy data, we show that the doldrums are largely confined between the edges of the ITCZ marked by enhanced surface convergence. While the region between the edges is a region of high time-mean precipitation, low wind speed events occur in the absence of precipitation. Based on these results, we hypothesize that low wind speed events occur in regions of low level divergence rather than convergence.

**Plain Language Summary** The doldrums, an area between the trade winds formerly feared by mariners because of its low wind speeds and variable wind directions, have largely disappeared from mention in the scientific literature. The most commonly given explanation for the existence of the doldrums, according to which the weaker surface winds result from the upward circulation of the trade winds, can only be true when averaged over timescales of days or weeks. In this study, we re-examine this region and its relationship to the convergence of the trade winds. We show that although low wind speed events occur in the region where the trade winds meet and precipitation rates are high on average, they occur precisely when there is no precipitation. This leads us to the hypothesis that these regions of low wind speeds are characterized by sinking rather than rising air.

## 1. Introduction

> "Day after day,
> day after day,
> We stuck, nor breath nor motion;
> As idle as a painted ship
> Upon a painted ocean"

is how S. T. Coleridge described the doldrums in the 1834 poem *The Rime of the Ancient Mariner*. Located between the trades, the doldrums were feared for their low wind speeds and variable wind directions by mariners when sailing ships were still the primary means of sea transportation (e.g., Maury, 1855). While still relevant to circumnavigators today (e.g., Herrmann & Wolfers, 2021), their decreasing economic importance went hand in hand with decreasing scientific interest and, until recently, mention of the doldrums had largely disappeared from the scientific literature. While no longer critical for trade, the doldrums have been suggested to be critical for correctly representing the tropical circulation systems in climate models (Klocke et al., 2017). Comparing simulations with and without parameterized convection over the tropical Atlantic, a key difference between the simulations were the significantly less pronounced doldrums in the simulation with parameterized convection. Given the central role of surface winds for convection, both thermodynamically (e.g., Emanuel, 1986) and dynamically (e.g., Zipser, 1977), Klocke et al. (2017) go so far as to speculate that this inability to correctly represent the doldrums might contribute to persistent biases in the representation of the Atlantic ITCZ (e.g., Siongco et al., 2015).

Due to their location between the trade winds, the doldrums have long been associated with the convergence of the trade winds in what is now known as the Intertropical Convergence Zone, ITCZ (Durst, 1926; Fletcher, 1945; Gentilli, 2005; Gordon, 1951). As the terms doldrums and ITCZ were used almost synonymously in the early

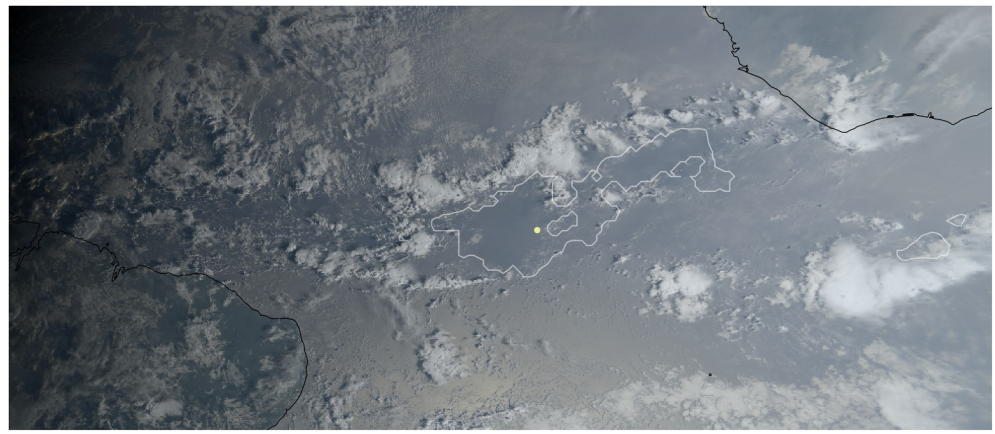

**Figure 1.** Natural color image of the Atlantic Intertropical Convergence Zone from NOAA Geostationary Operational Environmental Satellites 16 satellite on 4 February 2023 at 09:30 UTC. The solid white line indicates the 3 m $s^{-1}$ contour of the 10 m wind speed as measured by the Special Sensor Microwave Imager Sounder (4 February 2023; descending). The yellow dot denotes the position of RV Maria S. Merian.

literature, it is difficult to separate discussions of the ITCZ in general from discussions of the doldrums, especially their characteristic low wind speed events. For example, Durst (1926) describes the doldrums as a region within the equatorial trough with vanishing meridional pressure gradients, large-scale low-level convergence, and vertical ascent. He also notes that this region is characterized by strong and frequent precipitation. According to this description, low meridional wind speeds result from low-level convergence of the trade winds and low (geostrophic) zonal wind speeds result from the absence of a meridional pressure gradient. However, this description can only explain low wind speeds in the mean, that is, when averaged over time scales of days or weeks. At any given time, the ITCZ is characterized by rapid ascent through convective clouds but descent through the environment, which comprises the majority of the area even in regions of active convection (Riehl & Malkus, 1958; Yanai et al., 1973). As in the case of the convective updrafts, low-level convergence is usually highly localized, for example, in the form of convergence lines (Weller et al., 2017).

Recently Windmiller and Stevens (2024) showed that the Atlantic ITCZ has an inner life, that is, a rich dynamic and thermodynamic structure with substantial day-to-day variation. They found that the ITCZ is characterized by reduced meridional wind speeds between two edges of enhanced convergence. This raises the question of whether the doldrums mark the inner part of the ITCZ. This, at least, is what we observed during a recent campaign aboard the German RV Maria S. Merian in the boreal winter of 2023. During the campaign, three north-south transects of the East Atlantic ITCZ were completed and, as described in detail in Köhler et al. (2024), we observed regions of very low wind speeds between the edges of the ITCZ, as determined from the meridional wind speed component (Windmiller & Stevens, 2024). The wind speeds were particularly low during our last crossing, where the southern edge of the region of low wind speeds also marked the southern edge of the ITCZ, see Figure 1, with hourly mean wind speeds of about 1 m $s^{-1}$ at the time of the satellite image (see Supporting Information S1 for a movie version). The reduced wind speeds are actually visible as relatively dark regions on the natural color satellite image, because the low wind speeds lead to low wave heights (and sufficient distance from the point of specular reflection) leads to less scattering in the direction of the satellite (Cox & Munk, 1954).

In this study, we re-examine the doldrums and their day-to-day variation, focusing on their characteristic low wind speed events and how these relate to low-level convergence. To this end, we identify low wind speed events in reanalysis and buoy data as described in Section 2. We then investigate the relationship between low wind speed events and surface divergence on *multi-day timescales* in Section 3, *hourly timescales* in Section 4, and by considering the *temporal evolution* of low wind speed events in Section 5. In Section 6, we summarize our results and propose the hypothesis that the low wind speed events in the doldrums are caused by surface divergence and subsiding motion rather than surface convergence and ascending motion.

## 2. Data

To investigate the relationship between the ITCZ and the doldrums we use data from the Pilot Research Moored Array in the tropical Atlantic (PIRATA, Bourlès et al., 2008) as well as the fifth Generation of the ECMWF (European Centre for Medium-Range Weather Forecasts) Reanalysis of meteorological data (ERA5, Hersbach et al., 2018). To investigate the latitudinal and longitudinal dependence, we use three of the PIRATA buoys in the western Atlantic along 38°W (4°N, 8°N, 12°N) and three of the PIRATA buoys in the eastern Atlantic along 23°W (0°, 4°N, 12°N). The variables considered are air temperature (measured at a height of 3 m), precipitation (measured at a height of 3.5 m), wind speed (measured at a height of 4 m), and incoming short wave radiation (measured at a height of 3.5 m). We use data with the highest temporal resolution available, which corresponds to 10-min data for all variables considered. All measurements where the quality code indicated either "Lower Quality" (quality code 4) or "Sensor or Tube Failed" (quality code 5) were removed. All other data available at the time of analysis were used. The earliest data analyzed is from 01/30/1998 and the latest data is from 03/08/2018. For each buoy we have between 7.5 years (12°N 23°W) and 14.1 years (8°N 38°W) of data. To complement the buoy data, we use 20 years of hourly ERA5 data (horizontal resolution of $0.25° \times 0.25°$), from 18 August 2001 to 17 August 2021, centered at 38°W and 23°W and extending from 10°S to 20°N. To focus on the doldrums over the ocean, a land-sea mask was applied to mask all land grid cells. The variables we use are the hourly averaged precipitation rate, the vertically integrated total column water vapor, and the two 10 m horizontal wind components $\vec{v}_{10m}$. From the horizontal wind components we calculate the wind speed, $|\vec{v}_{10m}|$, and the divergence field, $\nabla \cdot \vec{v}_{10m}$, using metpy (version 1.4.1, May et al., 2016). For each of these fields, three-degree zonal averages are computed, centered on the longitudes of the buoys, that is, 39.5°W to 36.5°W and 24.5°W to 21.5°W.

In the following we investigate the relationship between the low wind speed events that characterize the doldrums and the surface convergence in the ITCZ. Low wind speed events are defined as extended and/or persistent regions of wind speeds less than 3 m $s^{-1}$. This threshold, previously used by Klocke et al. (2017), is also roughly equivalent to 5 knots, often stated as the minimum wind speed for sailing. For the buoy data, we require the wind speed to be below the threshold wind speed for at least 6 hours to classify as a low wind speed event. For the reanalysis data, we define a low wind speed event to occur at a given time and latitude whenever the three-degree zonally averaged wind speed is below the threshold wind speed. To calculate the mean occurrence rate of low wind speed events from the reanalysis data, we introduce a new binary field which indicates the presence (1) or absence (0) of a low wind speed event. Next, we investigate the relationship between low wind speed events and surface divergence on *multi-day timescales*, *hourly timescales*, and by considering the *temporal evolution* of the low wind speed events.

## 3. Multi-Day Timescales

### 3.1. Method

As discussed in the introduction, on time scales of days or weeks, we expect the low wind speed events to occur in the region of mean convergence that characterizes the ITCZ. To test this, we first compute 5-day averages (excluding the last day of the year if it is a leap year) for the low wind speed event field and the divergence field of the reanalysis data. For each 5-day interval, we then calculate the average over all years. In the thus averaged 10-m divergence field the region of mean convergence is defined as the region where the divergence is less than zero. As surface convergence is not the only way to identify the location of the ITCZ, we also use the column water vapor field and the precipitation field. Following Masunaga (2023), we use the 50 mm threshold in column water vapor to identify the edge of the ITCZ by the presence of a sharp gradient in moisture (Mapes et al., 2018; Masunaga & Mapes, 2020) and, following Wodzicki and Rapp (2016), we use a 2.5 mm $d^{-1}$ threshold in precipitation. We complement the seasonal cycle of low wind speed events in the reanalysis data with the corresponding frequency distribution of the low wind speed events captured by the PIRATA buoys.

### 3.2. Results

Figure 2 shows that the latitudinal extent of the East and West Atlantic doldrums has a seasonal cycle that follows the seasonal cycle of the ITCZ. This is shown by both the reanalysis and the buoy data. The region of mean low-level convergence defines a broad latitudinal band containing almost all low wind speed events. We find a similar agreement between the latitudinal extent of the ITCZ when determined by CWV or precipitation (not shown). In

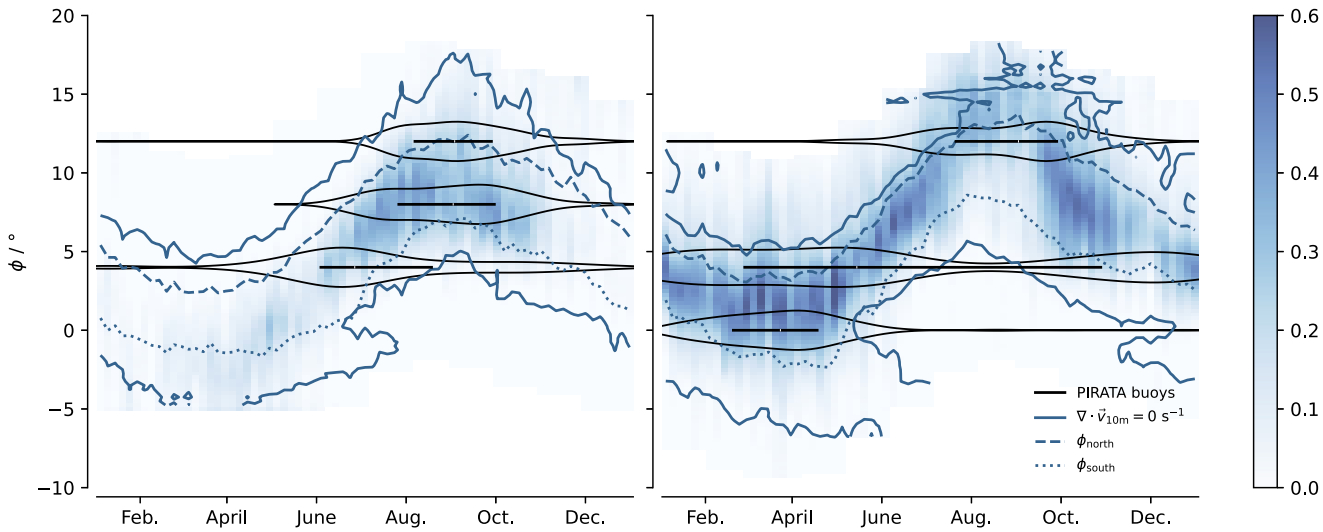


**Figure 2.** Seasonal cycle of the frequency of low wind speed events (left) around 38°W and (right) 23°W as calculated from reanalysis data (blue shading) and buoy data (black violins). The edges of the Intertropical Convergence Zone are shown as calculated from (solid blue line) zero divergence and (dashed blue line) the northern and (dotted blue line) southern convergence peaks (see Section 4.1).

addition to the latitudinal dependence, the frequency of occurrence of low wind speed events is also strongly dependent on the season and the region. Low wind speed events are generally more frequent in the eastern than in the western Atlantic. The frequency of low wind speed events in the west peaks during boreal summer, when the ITCZ is at it's northernmost position, while in the east it peaks during boreal spring, when the ITCZ is at it's southernmost position. Thus, while the ITCZ bounds the region in which low wind speed events occur throughout the year, the actual frequency of low wind speed events within the ITCZ depends on season and region. We next test the hypothesis that on short time scales, low wind speed events occur predominantly between the edges of the ITCZ.

## 4. Hourly Timescales

### 4.1. Method

We identify the edges of the ITCZ based on the hourly ERA5 surface convergence field $\left(-\nabla \cdot \vec{v}_{10m}\right)$ using a slightly modified version of the peak convergence strength method presented in Windmiller and Stevens (2024). To restrict ourselves to the ITCZ, we choose a dynamic latitude range that extends 10° north and 10° south of the latitude of the monthly precipitation maximum. For each instance in time we identify the latitudes of peak convergence, using the SciPy "find_peaks" function (version 1.8.1; Virtanen et al., 2020). To identify a local maximum in convergence as a peak, we set the required prominence and the height of the peaks to be equal to the 90th percentile of the convergence field calculated for all times and latitudes at the respective longitude. We then identify the northern and southern edges of the ITCZ as the latitude of the northernmost and southernmost convergence peak, respectively. To ensure that the outermost convergence lines related to the ITCZ are identified, this last step differs from the method described in Windmiller and Stevens (2024), where the edges were set equal to the two strongest convergence peaks. In the following analysis, we consider all cases where at least two convergence lines, and thus a northern and a southern ITCZ edge, are identified.

We first compare the 5-day mean of the northern and southern edges to the seasonal cycle of the frequency distribution of low wind speed events to test if the low wind speed events peak within the edges. We then assess the relationship between the low wind speed events and the ITCZ edges, by adjusting the latitudes of the low wind speed event field as well as the convergence field by

$$\phi_{\mathrm{adj}} = \left(\phi - \phi_{\mathrm{south}}\right)\frac{\left\langle \phi_{\mathrm{north}} - \phi_{\mathrm{south}} \right\rangle}{\phi_{\mathrm{north}} - \phi_{\mathrm{south}}} + \left\langle \phi_{\mathrm{south}} \right\rangle, \quad (1)$$

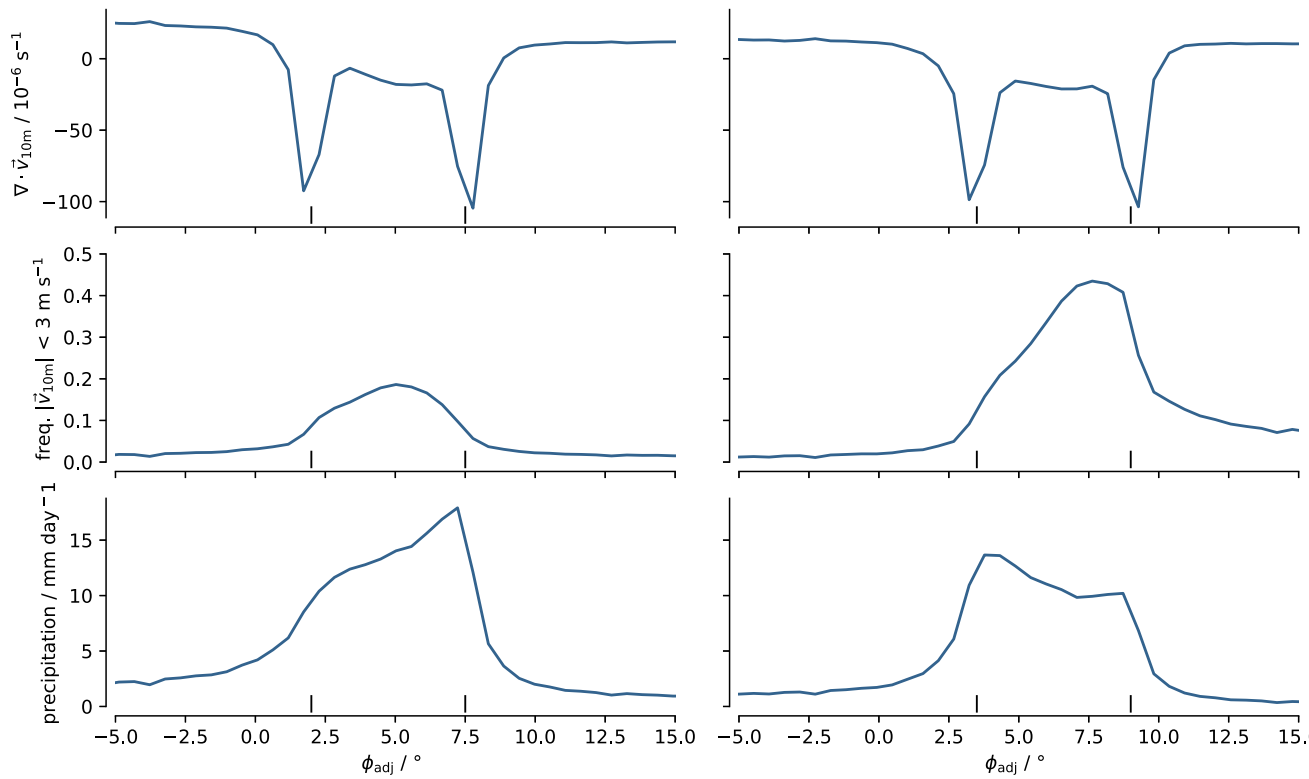


**Figure 3.** Zonal mean of the adjusted (top row) divergence field, (middle row) frequency of low wind speed events, and (bottom row) hourly averaged precipitation rate at (left) 38°W and (right) 23°W.

where $\phi_{south}$ is the southernmost and $\phi_{north}$ is the northernmost of the detected convergence peaks and $\langle \cdot \rangle$ denotes a temporal average over the whole data set. The rationale for this adjustment is to remove the smoothing of the dynamic and thermodynamic structure of the ITCZ that results from shifts in the latitudinal position and changes in the width of the ITCZ on seasonal but also sub-seasonal timescales.

### 4.2. Results

Two edges were detected in 70.2% of the cases in the western Atlantic and 72.6% of the cases in the eastern Atlantic. The 5-day mean of the northern and southern edges of the ITCZ shows that they closely match the edges of the doldrums (Figure 2). Figure 3 shows the low wind speed frequency together with the divergence and the precipitation field in the adjusted coordinates introduced in Equation 1. The divergence field in Figure 3 shows two pronounced convergence peaks, as expected from the design of the method. These convergence peaks correspond to the northern and southern edges of the latitudinal band with the highest frequency of low wind speed events as well as precipitation. While the distribution of low wind speed events in the western Atlantic is mostly symmetric with respect to the northern and southern convergence line, there is a marked asymmetry in the occurrence of low wind speed events in the eastern Atlantic with a pronounced peak close to $\phi_{north}$. This asymmetry is most pronounced during boreal summer (not shown). Interestingly, the precipitation field is also asymmetric. In the western Atlantic, precipitation peaks at the northern edge while in the eastern Atlantic precipitation peaks at the southern edge, though with a smaller secondary peak at the northern edge. Additional analysis shows that surface winds and fluxes are increased at, or close to, the edge with the higher precipitation rate, especially during the season of peak precipitation. East-west differences as well as seasonal differences in surface wind speed in the tropical Atlantic have previously been attributed to differences in sea surface temperature and pressure gradients (Hastenrath, 1991).

We tested the dependence of our results on the chosen threshold in prominence by changing it to the 80th percentile. In this case, we almost always detect at least two convergence peaks (94.7% in the western Atlantic and 96.0% in the eastern Atlantic). Figure 3 remains qualitatively the same, though the mean latitude of both the

northern and the southern edge of the ITCZ shifts poleward by about 1° and the increase of the various fields at the edges becomes less steep. To summarize, Figure 3 shows that low wind speed events occur primarily in the inner part of the ITCZ, answering the question about how the doldrums relate to the inner life of the Atlantic ITCZ.

## 5. Temporal Evolution

### 5.1. Method

Finally, we consider the relationship between convergence and the temporal evolution of low wind speed events using the buoy data. As we cannot calculate convergence from single point measurements, we use precipitation as a proxy for storm scale divergence and convergence. For individual storms, we expect low-level convergence to be associated with updraft formation and thus to precede precipitation formation, and low-level divergence to be associated with downdraft formation and thus to follow or coincide with precipitation formation (e.g., Byers & Braham, 1949). We address the question of whether the low wind speed events occur before or after the onset of precipitation by computing composites with respect to the onset ($t_{\text{onset}}$) and end time ($t_{\text{end}}$) of the low wind speed events. The onset time of the low wind speed event is defined as the first time the wind speed drops below the threshold wind speed, and the end time is the first time the wind speed rises above the threshold again. To use our composites to study both the onset and the end of the low wind speed events, we re-scale the time during the low wind speed events such that each event has the same duration, which we set to the median duration of all low wind speed events. To assess whether the precipitation rates before, during or after the low wind speed events are in general above or below average, we determine the month with the most frequent low wind speed events for each buoy and calculate the corresponding multiyear average precipitation rate for that month. This last step is necessary because the average precipitation rate observed at the buoys varies significantly throughout the year due to the seasonal cycle of the ITCZ. In general, this re-scaling is not limited to the wind speed or precipitation field, but can be applied to any other field. We will use this to investigate the temporal evolution of the surface (virtual) air temperature, where convective downdrafts manifest themselves in the form of temperature drops, and of shortwave radiation, where the presence of clouds leads to a reduction of incoming shortwave radiation at the surface compared to the top of the atmosphere. Therefore, as a rough indicator of the presence of clouds, we subtract the shortwave radiation measured at the buoys from the shortwave radiation at the top of the atmosphere as calculated following Hartmann (1994, p. 28).

### 5.2. Results

The mean time evolution of low wind speed events, as recorded by the PIRATA buoys, is shown in Figure 4. On average, about 400 low wind speed events are detected at each buoy with a median duration of 9 hr and 20 min. The number of detected events varies between 243 (23°W 12°N) and 511 (23°W 4°N) depending not only on the location of the buoy but also on the availability of data at that buoy. Considering all data available at the different buoys, low wind speed events occur only about 5% of the time. However, considering only the month with the most frequent low wind speed events at each buoy, low wind speed events occur about 15% of the time, varying between 9.6% (38°W 4°N) and 21.0% (23°W 12°N). For all considered variables, that is, surface wind speed, precipitation rate, air temperature, and the difference between top of the atmosphere and surface incoming shortwave radiation, the temporal evolution is at least qualitatively independent of the latitude and longitude of the buoys. Surface wind speeds are characterized by a slow decrease toward 3 m $s^{-1}$, our chosen wind speed threshold, until the onset of the low wind speed event, followed by a much faster decrease to around 1.5 m $s^{-1}$. The wind speed then remains at this level for the entire duration of the low wind speed event. Note that the close coincidence of wind speeds at around 1.5 m $s^{-1}$ is partly due to our method of detecting these events. Wind speeds are constrained to vary between 0 and 3 m $s^{-1}$, and values close to these limits are unlikely. This leads to wind speed distributions which peak close to the mean of the maximum and minimum value (not shown). The corresponding time evolution of precipitation shows average or above-average precipitation rates before the beginning and after the end of the low wind speed events, but a complete suppression during the low wind speed events.

As soon as the low wind speed event starts, the air temperature starts to slowly increase while the end of the low wind speed event is marked by a sudden drop in temperature. Additional analysis shows that the air-sea temperature before and after the low wind speed event is higher than the yearly averaged air-sea temperature difference. During the low wind speed event the air-sea temperature difference reduces to close or even increases

10.1029/2024GL109460

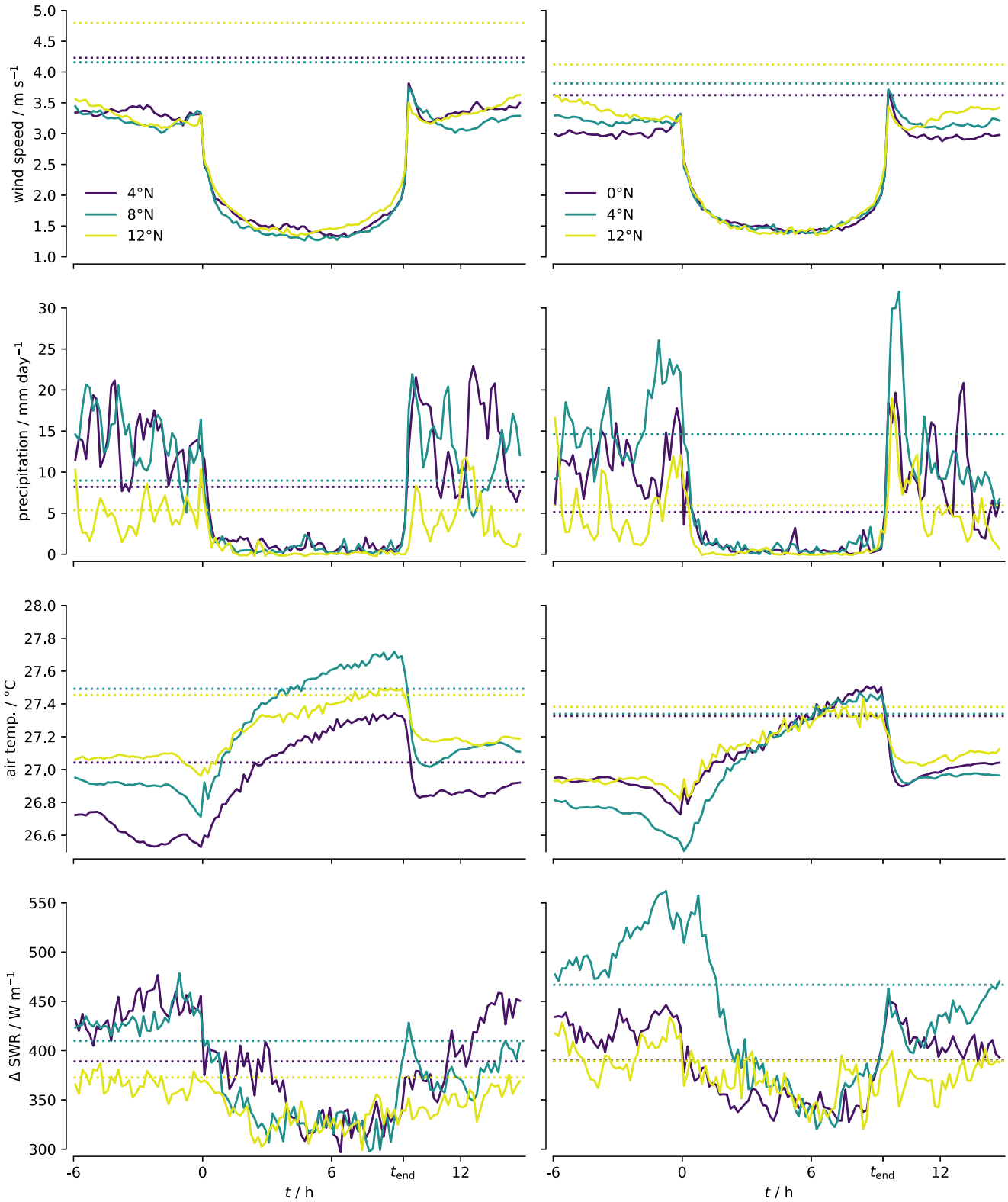


**Figure 4.** Time evolution of (top) surface wind speed, (second row) precipitation rate, (third row) surface air temperature, and (bottom row) top of the atmosphere shortwave radiation minus shortwave radiation as observed by the PIRATA buoys at (left) 38°W and (right) 23°W. The latitude of the buoy is indicated by the color. The time evolution is composited with respect to the onset and end time of the detected low wind speed events. The dotted lines show the monthly mean values during the month with the most frequent low wind speed events.

above the average difference. Given the low wind speed during the events, increased surface fluxes cannot explain the increase in temperature. One explanation is that in the absence of precipitation, evaporation can no longer cool the boundary layer and thus the temperature difference slowly increases towards the mean air-sea temperature difference. To investigate the role of humidity, we calculated the mixing ratio and the virtual temperature for the two buoys at which sea level pressure measurements and relative humidity measurements are available (23°W 0°, 23°W 12°N). We find only a small change in the mixing ratio for the different stages of the low wind speed events and the evolution of the virtual temperature is very similar to the evolution of the temperature, suggesting that the effect of humidity is small (not shown). Finally, we note that the difference between the top of atmosphere incoming shortwave radiation and the shortwave radiation measured at the surface tends to be reduced during the low wind speed event. As described above, this suggests that the cloud coverage during the low wind speed events is reduced, though the signal is less clear compared to the other variables. This increase in incoming shortwave radiation at the surface might also explain why we see a slow increase in the sea surface temperature during low wind speed events (not shown).

Taken together, these results suggest that the low wind speed events in the doldrums form in the wake of precipitating convection and end with the arrival of new precipitating convection. They are thus expected to be associated with divergence rather than convergence. With this in mind, it is interesting to return to Figure 1 and the corresponding time evolution shown in the Supporting Information S1. The movie version of the satellite image shows how the southern edge of the ITCZ, marked at times by an extended deep convective system, migrates southward over the location where we later detect the low wind speeds. We also note that once the low wind event fills most of the interior of the ITCZ, convection is largely confined to the edges of the ITCZ. This is reminiscent of edge-intensified convection in the ITCZ as described by Masunaga (2023).

## 6. Discussion and Conclusion

The doldrums, a region of low wind speeds and variable wind direction in the deep tropics, have been known for centuries, but until recently have largely disappeared from mention in the scientific literature. While the doldrums are commonly associated with the convergence of the trade winds in the ITCZ, the precise relationship is unknown. Defining the doldrums as the region of frequent low wind speed events, we show that on the timescale of multiple days the doldrums do in fact occur within the region of mean convergence that marks the ITCZ. The actual frequency of low wind speed events within the ITCZ is shown to depend on season and region.

Analysis of the relationship between low wind speed events and convergence on hourly time scales shows that low wind speed events peak inside the ITCZ, that is, inside the region bounded by enhanced convergence and characterized by increased precipitation. However, the composite evolution of low wind speed events shows that the onset of low wind speeds is actually marked by a sudden absence of precipitation as well as reduced surface air temperatures. Thus low wind speed events typically occur in between precipitation events in an otherwise high-precipitation region. While this may sound counterintuitive, it is important to remember that even in the moist tropics, updrafts and precipitation occupy only a small fraction of the area at any given time. Indeed, S. T. Coleridge appeared to be aware of this lack of precipitation, the poem with which this paper began continues:

> "Day after day, day after day,
> We stuck, nor breath nor motion;
> As idle as a painted ship
> Upon a painted ocean.
> Water, water, every where,
> And all the boards did shrink;
> Water, water, every where,
> Nor any drop to drink."

Based on the result that the low wind speed events occur between the edges of the ITCZ and between precipitation events, we hypothesize that the low wind speed events in the doldrums are not related to surface convergence and ascending air masses, but rather to surface divergence and descending air masses. Low wind speeds would then result from low-level surface divergence opposing the low-level inflow from the trade winds. Surface divergence could result from several processes, in particular it could be driven by gravity wave induced subsidence (Bretherton & Smolarkiewicz, 1989) or by surface density currents (e.g., Benjamin, 1968). Atmospheric surface

density currents can, for example, be precipitation-driven through evaporation or condensate loading (e.g., Byers & Braham, 1949) or radiation-driven (Coppin & Bony, 2015). Testing this hypothesis requires an analysis of the relationship between low wind speed events and vertical velocity profiles to first verify whether low wind speed events are indeed related to subsidence and surface divergence, and if so, to determine what causes this surface divergence. Since the vertical structure of vertical motions in reanalyses can be highly biased (e.g., Huaman et al., 2022), this investigation is beyond the scope of the present study. One possibility to investigate this hypothesis will be to use cloud-resolving simulations in realistic setups, another might be to use idealized simulations. In the case of self-aggregation, for example, we have shown that the self-aggregation cluster, that is, the region of increased mean precipitation bounded by intense convergence, is characterized by reduced surface wind speeds within (Windmiller & Hohenegger, 2019). In parallel to investigating this question using atmospheric models, we are also planning to investigate the low wind speed events in the doldrums using observational data collected specifically for this purpose. The relationship between low wind speed events and the area-averaged mesoscale circulation properties of vertical velocity and divergence (Bony & Stevens, 2019; George et al., 2021) within the ITCZ will be analyzed with the data collected during the upcoming ORCESTRA campaign. ORCESTRA is planned for August and September 2024 with the goal to deepen our understanding of the drivers and effects of mesoscale organization on small and large scales with a particular focus on the doldrums.

## Data Availability Statement

All data used in this study is publicly available. NOAA Geostationary Operational Environmental Satellites 16, 17, and 18 was accessed on 2024-02-17 from https://registry.opendata.aws/noaa-goes. Special Sensor Microwave Imager Sounder data (Wentz et al., 2012) was downloaded using NASA's Earth Observing System Data and Information System. The data from the Pilot Research Moored Array in the tropical Atlantic (Bourlès et al., 2008) was downloaded from https://www.pmel.noaa.gov/tao/drupal/disdel/. The ERA5 data (Hersbach et al., 2018) was downloaded from the Copernicus Climate Change Service (C3S) Climate Data Store. The results contain modified Copernicus Climate Change Service information 2021. Neither the European Commission nor ECMWF is responsible for any use that may be made of the Copernicus information or data it contains.

**Acknowledgments**
The author thanks Geet George, Cathy Hohenegger, Divya Sri Praturi, Martin Singh, and Bjorn Stevens for helpful discussions. The author would like to further thank Martin Singh for suggesting and sending a printed copy of "The Rime of the Ancient Mariner" by S. T. Coleridge. Finally, the author thanks Hirohiko Masunaga and Ingo Richter for their helpful reviews, which significantly improved the quality of the article. The author acknowledges the public support of the conducted basic research through the Max Planck Society. Open Access funding enabled and organized by Projekt DEAL.

## References

Benjamin, T. B. (1968). Gravity currents and related phenomena. *Journal of Fluid Mechanics*, *31*(2), 209–248. https://doi.org/10.1017/S0022112068000133

Bony, S., & Stevens, B. (2019). Measuring area-averaged vertical motions with dropsondes. *Journal of the Atmospheric Sciences*, *76*(3), 767–783. https://doi.org/10.1175/JAS-D-18-0141.1

Bourlès, B., Lumpkin, R., McPhaden, M. J., Hernandez, F., Nobre, P., Campos, E., et al. (2008). The Pirata program: History, accomplishments, and future directions [Dataset]. *Bulletin of the American Meteorological Society*, *89*(8), 1111–1126. https://doi.org/10.1175/2008BAMS2462.1

Bretherton, C. S., & Smolarkiewicz, P. K. (1989). Gravity waves, compensating subsidence and detrainment around cumulus clouds. *Journal of the Atmospheric Sciences*, *46*(6), 740–759. https://doi.org/10.1175/1520-0469(1989)046⟨0740:GWCSAD⟩2.0.CO;2

Byers, H. R., & Braham, R. R. (1949). The thunderstorm: Report of the thunderstorm project (a joint project of four U.S. Government Agencies: Air Force, Navy, National Advisory Committee for Aeronautics, and Weather Bureau) (Tech. Rep.). https://doi.org/10.1002/qj.49707733225

Coppin, D., & Bony, S. (2015). Physical mechanisms controlling the initiation of convective self-aggregation in a General Circulation Model. *Journal of Advances in Modeling Earth Systems*, *7*(4), 2060–2078. https://doi.org/10.1002/2015MS000571

Cox, C., & Munk, W. (1954). Measurement of the roughness of the sea surface from photographs of the Sun's Glitter. *Journal of the Optical Society of America*, *44*(11), 838. https://doi.org/10.1364/JOSA.44.000838

Durst, C. S. (1926). The doldrums of the Atlantic. *Geophysical Memoirs*, *28*, 229–237.

Emanuel, K. A. (1986). An air-sea interaction theory for tropical cyclones. Part I: Steady-state maintenance. *Journal of the Atmospheric Sciences*, *43*(6), 585–605. https://doi.org/10.1175/1520-0469(1986)043⟨0585:AASITF⟩2.0.CO;2

Fletcher, R. D. (1945). The general circulation of the tropical and equatorial atmosphere. *Journal of Meteorology*, *2*(3), 167–174. https://doi.org/10.1175/1520-0469(1945)002⟨0167:TGCOTT⟩2.0.CO;2

Gentilli, J. (2005). Doldrums. In J. E. Oliver (Ed.), *Encyclopedia of world climatology* (p. 338). Springer. (Series Title: Encyclopedia of Earth Sciences Series). https://doi.org/10.1007/1-4020-3266-8_69

George, G., Stevens, B., Bony, S., Pincus, R., Fairall, C., Schulz, H., et al. (2021). JOANNE: Joint dropsonde Observations of the Atmosphere in tropical North atlaNtic meso-scale Environments. *Earth System Science Data*, *13*(11), 5253–5272. https://doi.org/10.5194/essd-13-5253-2021

Gordon, A. H. (1951). Seasonal variation of the axes of low-latitude pressure and divergence patterns over the oceans. *Quarterly Journal of the Royal Meteorological Society*, *77*(332), 302–306. https://doi.org/10.1002/qj.49707733215

Hartmann, D. L. (1994). *Global physical climatology* (Vol. 56). Academic Press.

Hastenrath, S. (1991). Regional circulation systems. In *Climate dynamics of the tropics* (pp. 114–218). Springer Netherlands. https://doi.org/10.1007/978-94-011-3156-8_6

Herrmann, B., & Wolfers, A. (2021). *Allein zwischen Himmel und Meer: meine achtzig Tage beim härtesten Segelrennen der Welt*. C. Bertelsmann.

Hersbach, H., Bell, B., Berrisford, P., Biavati, G., Horányi, A., Muñoz Sabater, J., et al. (2018). ERA5 hourly data on single levels from 1959 to present [Dataset]. *Copernicus Climate Change Service (C3S) Climate Data Store (CDS)*. https://doi.org/10.24381/cds.adbb2d47

Huaman, L., Schumacher, C., & Sobel, A. H. (2022). Assessing the vertical velocity of the East Pacific ITCZ. *Geophysical Research Letters*, *49*(1), e2021GL096192. https://doi.org/10.1029/2021GL096192

Klocke, D., Brueck, M., Hohenegger, C., & Stevens, B. (2017). Rediscovery of the doldrums in storm-resolving simulations over the tropical Atlantic. *Nature Geoscience*, *10*(12), 891–896. https://doi.org/10.1038/s41561-017-0005-4

Köhler, L., Windmiller, J., Baranowski, D., Brennek, M., Ciuryło, M., Hayo, L., et al. (2024). Calm Ocean, stormy sea: Atmospheric and oceanographic observations of the Atlantic during the arc ship campaign. *Earth System Science Data Discussions*, *2024*, 1–32. https://doi.org/10.5194/essd-2024-275

Mapes, B. E., Chung, E. S., Hannah, W. M., Masunaga, H., Wimmers, A. J., & Velden, C. S. (2018). The meandering margin of the meteorological moist tropics. *Geophysical Research Letters*, *45*(2), 1177–1184. https://doi.org/10.1002/2017GL076440

Masunaga, H. (2023). The edge intensification of eastern Pacific ITCZ convection. *Journal of Climate*, *36*(10), 3469–3480. https://doi.org/10.1175/JCLI-D-22-0382.1

Masunaga, H., & Mapes, B. E. (2020). A mechanism for the maintenance of sharp tropical margins. *Journal of the Atmospheric Sciences*, *77*(4), 1181–1197. JAS–D–19–0154.1. https://doi.org/10.1175/jas-d-19-0154.1

Maury, M. F. (1855). *The physical geography of the sea*. Sampson, Low, Son & Co. https://doi.org/10.5962/bhl.title.102148

May, R., Arms, S., Marsh, P., Bruning, E., Leeman, J., Bruick, Z., & Camron, M. D. (2016). MetPy: A Python package for meteorological data [Object]. https://doi.org/10.5065/D6WW7G29

Riehl, H., & Malkus, J. S. (1958). On the heat balance in the equatorial trough zone. *Geophysica*, *6*(2), 503–538.

Siongco, A. C., Hohenegger, C., & Stevens, B. (2015). The Atlantic ITCZ bias in CMIP5 models. *Climate Dynamics*, *45*(5), 1169–1180. https://doi.org/10.1007/s00382-014-2366-3

Virtanen, P., Gommers, R., Oliphant, T. E., Haberland, M., Reddy, T., Cournapeau, D., et al. (2020). SciPy 1.0: Fundamental algorithms for scientific computing in Python. *Nature Methods*, *17*(3), 261–272. https://doi.org/10.1038/s41592-019-0686-2

Weller, E., Shelton, K., Reeder, M. J., & Jakob, C. (2017). Precipitation associated with convergence lines. *Journal of Climate*, *30*(9), 3169–3183. https://doi.org/10.1175/JCLI-D-16-0535.1

Wentz, F., Hilburn, K., & Smith, D. (2012). RSS SSMIS ocean product grids daily from DMSP F17 netCDF [Dataset]. https://doi.org/10.5067/MEASURES/DMSP-F17/SSMIS/DATA301

Windmiller, J. M., & Hohenegger, C. (2019). Convection on the edge. *Journal of Advances in Modeling Earth Systems*, *11*(12), 3959–3972. https://doi.org/10.1029/2019MS001820

Windmiller, J. M., & Stevens, B. (2024). The inner life of the Atlantic Intertropical Convergence Zone. *Quarterly Journal of the Royal Meteorological Society*, *150*(758), 523–543. https://doi.org/10.1002/qj.4610

Wodzicki, K. R., & Rapp, A. D. (2016). Long-term characterization of the Pacific ITCZ using TRMM, GPCP, and ERA-Interim. *Journal of Geophysical Research: Atmospheres*, *121*(7), 3153–3170. https://doi.org/10.1002/2015JD024458

Yanai, M., Esbensen, S., & Chu, J. (1973). Determination of bulk properties of tropical cloud clusters from large-scale heat and moisture budgets. *Journal of the Atmospheric Sciences*, *30*(4), 611–627. https://doi.org/10.1175/1520-0469(1973)030<0611:dobpot>2.0.co;2

Zipser, E. J. (1977). Mesoscale and convective–scale downdrafts as distinct components of squall-line structure. *Monthly Weather Review*, *105*(12), 1568–1589. https://doi.org/10.1175/1520-0493(1977)105⟨1568:MACDAD⟩2.0.CO;2